All-fiber laser with intracavity acousto-optic dynamic mode converter for efficient generation of radially polarized cylindrical vector beams

L. Carrión-Higueras, E. P. Alcusa-Sáez, A. Díez, M. V. Andrés

Departamento de Física Aplicada-ICMUV, Universidad de Valencia, Dr. Moliner 50, 46100, Spain

Abstract: We report an all-fiber laser that emits a radially polarized cylindrical vector beam (CVB) at 1 μm based on an intracavity acousto-optic mode converter. We efficiently generate the CVB taking advantage of the acousto-optic coupling from the HE_{11} mode to the TM_{01} mode in a two-mode fiber. The laser can be switched from emitting a Gaussian–like beam to a radially polarized CVB. Radially polarized CVBs with modal and polarization purities > 98 % and a maximum power of 65 mW were generated.

Index Terms: Fiber Laser; cylindrical vector beams, radial polarization.

1. Introduction

Cylindrical vector beams (CVBs) are vector-beam solutions of Maxwell's equations with axial symmetry in both amplitude and phase [1], [2]. They are spatially variant polarization beams that exhibit cylindrical symmetry in polarization. Specifically, CVBs with radial polarization have raised considerable attention due to their unique properties. A variety of applications arising from the tight focusing capability [3] and the special polarization distribution has been demonstrated. Radially polarized CVBs have shown advantages against other polarization beams in, for instance, materials processing [4], [5], optical trapping of particles [6], [7], and high-resolution microscopy [8], [9]. Special light beams as CVBs and beams carrying orbital angular momentum [10] have risen also an interest for mode-division and space-division multiplexing [11].

Various methods of generating radially polarized beams have been reported. Most passive methods convert spatially invariant polarization beams into CVBs by the use of spatially variant phase elements [12]. Active methods involve the use of laser intracavity components that force the laser to emit CVBs [13], [14]. Generation of CVBs with few-mode optical fibers deserves special attention. Optical fibers are a good platform since some fiber eigenmodes exhibit the properties of CVBs. Although the generation of CVBs based on illuminating a few-mode optical fiber with a modified beam is achievable [15], the most efficient methods involve inducing the appropriate mode transformation in the fiber itself by using either fiber Bragg gratings [16], [17], periodic microbending [18] or waveguide transitions [19]. In standard optical fibers the first high-order mode group comprises the almost degenerate azimuthally TE_{01} and radially TM_{01} polarized beams, as well as two strictly degenerate states of the HE_{21} mode. Most of the excitation methods used in the past are not able to excite each mode individually in a controlled manner. This problem can be overcome, for example, by the use of specialty optical fibers with specific refractive index profiles to lift the near-degeneracy of the bunch of modes [20]. Alternatively, TE_{01} and TM_{01} modes can be selectively excited in standard few-mode optical fibers by acousto-optic interaction using flexural elastic waves [21]. A flexural elastic wave propagating in a fiber creates a periodic refractive-index perturbation with similar transversal profile than periodic microbending [18], but with the advantage of being dynamically tunable in both strength and periodicity. More important, the length of the elastically-induced grating (only limited by attenuation) can be of several tens of cm. This feature enables the selective excitation of each of the three modes (TE_{01}, TM_{01}, HE_{21}) since the coupling bandwidth is inversely proportional to the interaction length. A theoretical discussion about the mechanism of the vector modes coupling induced by flexural elastic waves can be found in [22].

In the last years, there has been an increasing activity in the development of fiber laser CVB sources. In many fiber laser cavity designs, bulk optical elements and free-space propagation are present [13], [14], which are the origin of high cavity losses, and consequently, of low laser efficiency. The use of bulk components in combination with single-mode optical fibers requires fine alignment and good mechanical stability, which complicates the design of practical devices. Few all-fiber laser schemes have also been reported. In most of them, intracavity mode conversion from the fundamental mode to cylindrically polarized modes relies on a lateral core-offset splice between a single-mode and a two-mode fiber [23], [24], [25].

In this paper, we report an all-fiber laser that emits a radially polarized CVB at 1 μm based on an intracavity acousto-optic dynamic mode converter. The acousto-optic interaction provides full control on the performance of the mode converter. The laser can be switched from emitting a Gaussian-like beam profile corresponding to the fundamental fiber mode to a radially polarized CVB in a very simple and fast way. Although in our present setup the optical gain is provided by amplification of

the fundamental fiber mode and the average power is moderate, this work is an advance towards fiber-based high power CVB lasers systems.

2. 2. Experimental results and discussion

2.1. Performance of the acousto-optic mode converter

The acousto-optic mode converter (AO-MC) was implemented using 50 cm of SM2000 fiber (nominal λc = 1.7 μm and NA = 0.12) commercialized by Thorlabs Inc. We chose this fiber for two reasons: (1) the cutoff is far from the laser emission wavelength so that ensures strong guidance of the vector modes (TE_{01}, TM_{01}, HE_{21}), and (2) the phase-matching condition for the coupling between the fundamental mode and the vector modes at wavelengths around 1 μm is achieved at a lower RF frequency compared to other standard fibers [21], making more efficient the generation of elastic waves with the required amplitude. Flexural elastic waves were generated by a thickness-mode piezoelectric transducer driven by an RF signal generator, and were launched along the fiber via a horn. A mode stripper was inserted at the input to ensure that light enters the mode converter in the fundamental mode.

Figure 1 shows the results of the experimental characterization of the acousto-optic mode converter. Inset of Fig. 1 shows a representative transmittance spectrum obtained with broadband unpolarized light. For this characterization, a second mode stripper was inserted at the output of the acousto-optic interaction fiber section to transform the coupling from the fundamental mode to a high-order mode into a notch. Three notches are observed, they result from coupling between the fundamental mode and the triplet of modes (TE_{01}, TM_{01}, HE_{21}). The measured center wavelengths of each coupling as a function of acoustic frequency are shown, the resonance wavelengths shift to longer wavelengths as the acoustic frequency increases. At this point, we find interesting to discuss Fig. 1(a) in some detail. The relative position of the curves corresponding to modes TE_{01}, HE_{21}, TM_{01} is determined by the modal index difference with respect to the fundamental mode. According to a step-index model, the curves of modes TM_{01} and TE_{01} should be interchanged, while in our experiments it is definitely demonstrated that modes are as depicted in Fig. 1(a) (e. g., see Fig. 4). This is related to the fact that the cutoff wavelength of TM_{01} and TE_{01} modes is not degenerate in fibers with a smooth index profile (rather than an ideal step-index), as it was demonstrated in earlier theoretical analysis [26]. There is a wavelength range in which the refractive index difference with respect to the fundamental mode is rather different from what a simple step-index model predicts. These fine details of the vector modes are not usually discussed, nor reported, but are crucial when designing a CVB source based on optical fibers.

Figure 1(b) shows the transmittance spectrum measured with polarized light and the input polarization state was adjusted to optimize the coupling to the radially polarized TM_{01} mode. The transmission notch is ~20 dB in depth (this value is probably limited by the performance of the mode strippers) which indicates a mode conversion of ~ 99 %. Thus, the mode conversion efficiency could be dynamically varied from 0% to 99% through the RF voltage amplitude.

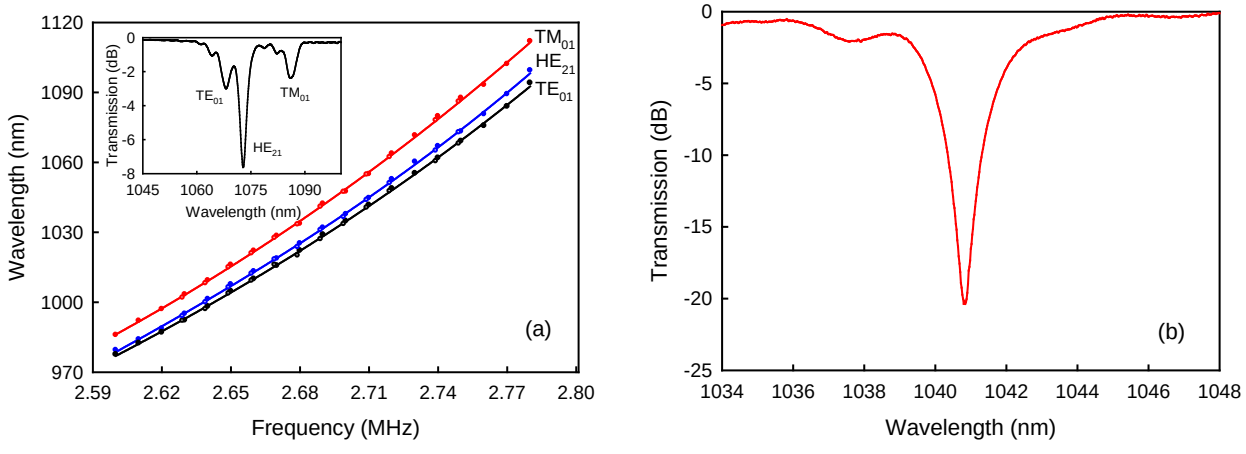

Fig. 1. (a) Acousto-optic resonance wavelength versus RF frequency. Inset: transmittance spectrum measured using an ASE light source (RF frequency: 2.749 MHz). (b) Transmittance spectrum measured with linearly polarized light and input polarization state adjusted to optimize coupling to the TM_{01} mode. Optimum HE_{11}-TM_{01} coupling is achieved when the linear polarization orientation of the HE_{11} mode is parallel to the vibration directions of the acoustic flexural wave [22]. RF frequency: 2.687 MHz; RF voltage: 45 V_{pp}.

2.2. Laser setup and emission characteristics

A schematic diagram of the fiber laser is shown in Fig. 2. All fibers are single-mode at the emission wavelength except the section used in the AO-MC. The gain was provided by 60 cm of single-clad, polarization maintaining Yb-doped fiber (Nufern PM-YSF-HI) that was pumped at 980 nm through a fiber polarization maintaining (PM) wavelength division multiplexer. The PM polarizer filters the fast-axis mode and guarantees that linearly polarized light is delivered to the mode converter. The PC was inserted to adjust the polarization of the light at the input of the mode converter and was mounted using non-PM

fiber. Special care was taken when making the fusion splice between the PC's single-mode fiber and the two-mode fiber of the mode converter to avoid misalignment of the fiber cores in order to minimize the excitation of the high-order modes in the two-mode fiber. Additionally, the mode stripper guarantees that high-order modes are stripped out of the core. Feedback of the amplified signal was produced by an FBG written in PM fiber (Bragg wavelength: 1040.8 nm; reflectivity > 99 %) and the Fresnel reflection from a perpendicular fiber cleave, from which the output was taken. By monitoring the signal coming out from the FBG, it was checked that laser emission was suppressed when the perpendicularly cleaved fiber end (see Fig. 2) was immersed in index matching oil, which confirms that the AO-MC was part of the laser resonant cavity. Finally, images of the output beam intensity pattern at different experimental conditions were recorded using an aspheric lens (× 30) and a CCD camera.

Figure 3 shows the characteristics of the output beam for three different RF voltage levels. Inset of Fig. 3 shows images of the beam intensity distribution. The linear profiles are intensity distribution across the beam center along the horizontal axis. When no voltage is applied to the piezoelectric transducer, the laser emits a gaussian-like beam, as expected, corresponding to the fundamental fiber mode. As the RF voltage was increased, the intensity beam profile evolves to a more complex structure as a result of the superposition of the two different beam profiles. For the optimum voltage level, i.e. when highest mode conversion efficiency is achieved, the beam shows a pronounced doughnut-shaped pattern, characteristic of a CVB.

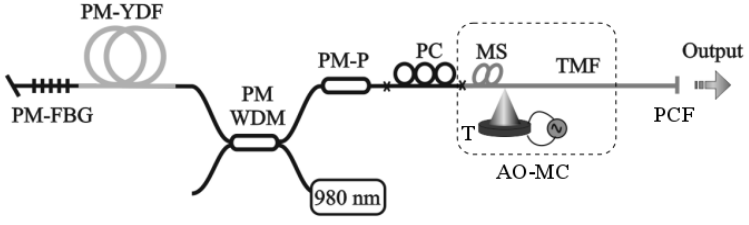

Fig. 2. Diagram of the fiber laser set-up. TMF: two-mode fiber; MS: mode stripper; PC: polarization controller; PM-WDM: polarization maintaining wavelength-division multiplexer; PM-P: fiber polarizer with input and output polarization maintaining fibers; PM-FBG: fiber Bragg grating written in single-mode PM fiber; PM-YDF: polarization maintaining Ytterbium doped fiber; T: piezoelectric transducer; AO-MC: acousto-optic mode converter; PCF: perpendicularly cleaved fiber.

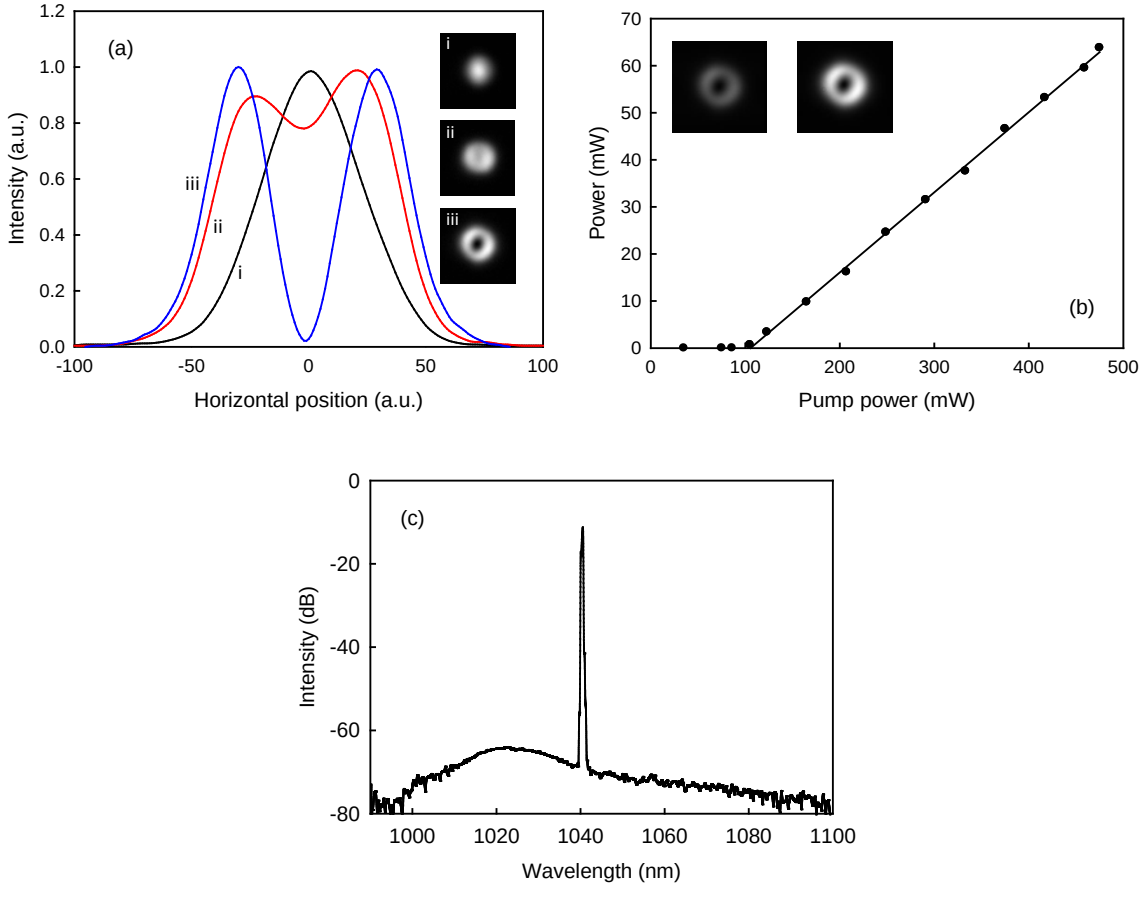

Fig. 3. (a) Intensity distribution across the beam center along the horizontal axis, for RF voltage amplitude: (i) 0 V_{pp}, (ii) 18 V_{pp}, (iii) 45 V_{pp}. Inset: corresponding beam intensity patterns (pump power: 475 mW). (b) Laser output power as a function of pump power. Insets: images of the intensity beam pattern at 123 mW (left) and 475 mW (right). (c) Laser spectrum at 475 mW pump power.

The laser output power as a function of pump power, when the laser was emitting with the TM_{01} mode, is shown in Fig. 3(b). The laser threshold is 100 mW, the efficiency is 13.5 %, and the maximum power emitted was 65 mW. It is worth to note that very similar figures were obtained when the laser emitted in the gaussian-like beam mode, which indicates that the AO coupling process taking place in the mode converter did not add noticeable insertion losses to the laser cavity. The output beam intensity patterns just above threshold, and at the maximum pump power, are shown in Fig. 3(b). It can be concluded that mode purity was preserved across the whole pump power range. Figure 3(c) shows the spectrum of the laser at the highest pump power measured by an OSA. The linewidth is narrower than 50 pm (which is the effective spectral resolution of our OSA) and signal-to-ASE ratio, integrated over the whole wavelength range, is larger than 99.9%.

The polarization characteristics of the CVB were analyzed with a linear polarizer. The intensity distributions after passing through the polarizer with different transmission axis orientations are shown in Fig. 4 (b)-(d). The white arrow indicates the orientation of the transmission axis of the polarizer. The symmetric two-lobe-structured intensity distribution parallel to the transmission axis of the polarizer confirms that the output beam corresponds to the radially polarized TM_{01} mode. The polarization purity was investigated by analyzing the intensity profile of the two-lobe beam at a radius r as a function of the azimuthal angle θ (Fig. 5(a)). Experimental intensity data were extracted from the intensity pattern image shown in the inset. For a pure radially polarized beam, the intensity at an arbitrary radius r and azimuthal angle θ is given by $I(r,\theta) = I_{max}(r)\cdot\cos^2(\theta - \theta_0)$ where θ_0 is the angle orientation of the transmission axis of the linear polarizer. The polarization extinction ratio (PER = I_{max}/I_{min}) was measured to be > 98 %, confirming high radial-polarization purity for the output beam.

Analysis of the laser emission mode purity, i.e. fractional content of TM_{01} mode versus fundamental mode, was performed by evaluating one-dimensional intensity distributions across the center of the beam. Figure 5(b) shows the intensity profile corresponding to the beam shown in Fig. 4 (a). Although the doughnut-shape intensity profile is clear, some residual intensity at the center of the beam indicates there is emission in the form of the fundamental mode. The measured intensity profile was fitted by a linear superposition of the intensity profiles of HE_{11} and TM_{01} modes, that were calculated theoretically using the nominal characteristics of the SM2000 fiber. A scale factor was applied to the horizontal position to match calculated and experimental profiles. The best fit is included in Fig. 5(b), the power ratio of TM_{01} to fundamental mode is 55:1, which indicates a TM_{01} mode purity of 98.2 %. The presence of the fundamental mode can be attributed to the lack of full mode conversion efficiency. Additionally, amplified spontaneous emission at wavelengths outside the AO coupling bandwidth, for which the mode converted does not act, can also contribute to this noise floor.

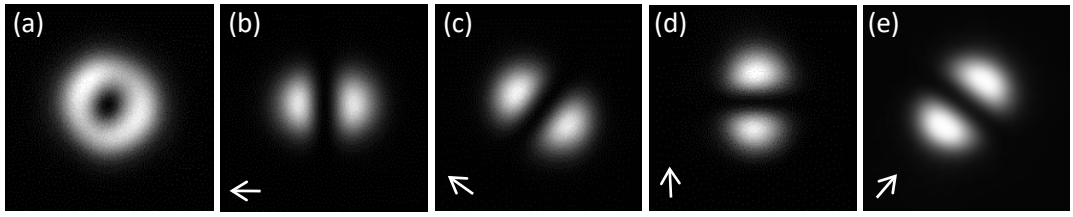

Fig. 4. Image of (a) the output beam intensity pattern, and (b)-(e) after passing through a linear polarizer with transmission axes orientation indicated by the arrows. Pump power: 460 mW

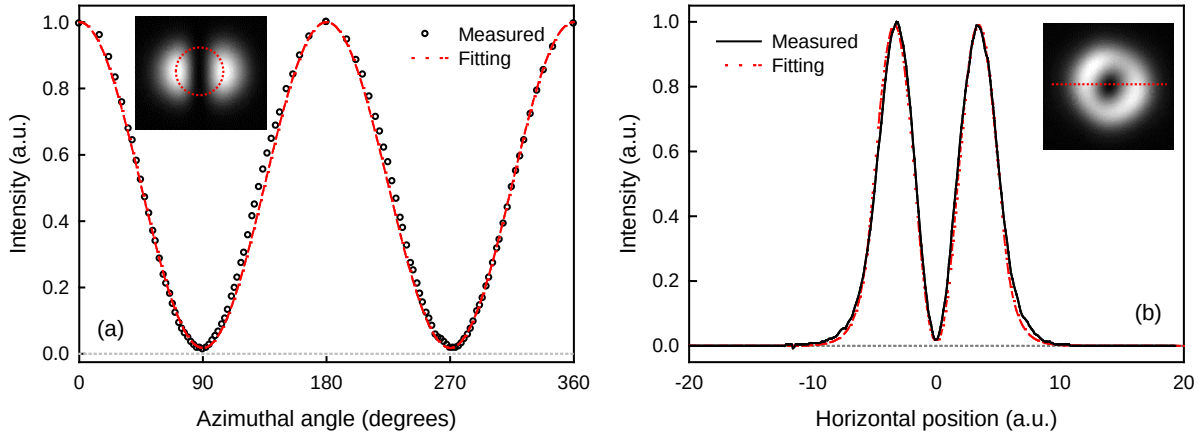

Fig. 5. (a) Azimuthal-intensity profile for radius r of the beam after passing through a horizontally oriented polarizer. (b) Intensity distribution across the beam center along the horizontal axis.

Finally, we would like to point out that the laser showed a good temporal stability in terms of emitted power and beam profile, at least during few hours. To this respect, it is worth to note that the good stability of the laser is, to a great extent, due to the use of PM fibers plus the polarizer, which avoided gain competition of the two linear polarization states of the fundamental mode. In fact, we arranged an equivalent laser setup with no-PM fibers. In that case, we achieved emission of

CVBs as in the prototype reported in this work but the temporal stability of the emission was significantly poorer. It is worth to note that, in our present arrangement, the polarization controller prior to the AO-MC could be removed from the laser setup if the axes of the PM fiber were oriented precisely with respect to the vibrating plane of the acoustic wave.

Generation of azimuthally polarized CVB using the same laser arrangement could also be observed. However, the modal and polarization purities in this case were not as good as for the radially polarized beams. We believe that the origin of this limitation is that the acousto-optic resonance wavelengths for TE_{01} and HE_{21} modes are extremely close for this two-mode optical fiber in the wavelength range of interest, which makes difficult the selective excitation of the TE_{01} mode.

4. Conclusions

We have demonstrated an all-fiber laser that emits a high purity radially polarized CVB. Intracavity mode conversion from the fundamental HE_{11} mode to the radially polarized TM_{01} mode is achieved by acousto-optic interaction in a two-mode fiber. This mode converter in combination with PM active fiber provides good temporal stability, which is a significant step towards fiber-based robust and practical CVB sources. In addition, the dynamic nature of the mode converter allows switching the emission of the laser from a gaussian-like beam to the radially polarized CVB. The all-fiber laser emitted radially polarized CVB with modal and polarization purity > 98 %. The efficiency of the laser was 13.5 %, and the maximum power emitted was 65 mW. We have discussed also some fine details of the TM_{01} and TE_{01} dispersion curves that are definitely relevant for the design of fiber-based CVB light sources.

Acknowledgements

This research was supported financially by the Ministerio de Economia y Competitividad of Spain and FEDER (TEC2013-46643-C2-1-R) and the Generalitat Valenciana (PROMETEOII /2014/072).

References

[1] D. G. Hall, "Vector-beam solutions of Maxwell's wave equation," Opt. Lett. vol. 21, pp. 9-11, 1996.
[2] Q. Zhan, "Cylindrical vector beams: from mathematical concepts to applications," Adv. Opt. Photon., vol. 1, pp. 1-57, 2009.
[3] R. Dorn, S. Quabis, and G. Leuchs, "Sharper focus for a radially polarized light beam," Phys. Rev. Lett., vol. 91, 233901, 2003.
[4] V. G. Niziev and A. V. Nesterov, "Influence of beam polarization on laser cutting efficiency," J. Phys. D: Appl. Phys., vol. 32, pp. 1455-1461, 1999.
[5] M.Meier, V. Romano, and T. Feurer, “Material processing with pulsed radially and azimuthally polarized laser radiation,” Appl. Phys. A, vol. 86, pp. 329–334, 2007.
[6] M. G. Donato, S. Vasi, R. Sayed, P. H. Jones, F. Bonaccorso, A. C. Ferrari, P. G. Gucciardi, and O. M. Maragò, "Optical trapping of nanotubes with cylindrical vector beams," Opt. Lett., vol. 37, pp. 3381-3383, 2012.
[7] Y. Kozawa and S. Sato, "Optical trapping of micrometer-sized dielectric particles by cylindrical vector beams," Opt. Express, vol. 18, pp. 10828-10833, 2010.
[8] Wai Teng Tang, Elijah Y. S. Yew, and Colin J. R. Sheppard, "Polarization conversion in confocal microscopy with radially polarized illumination," Opt. Lett., vol. 34, pp. 2147-2149, 2009.
[9] Fake Lu, Wei Zheng, and Zhiwei Huang, "Coherent anti-Stokes Raman scattering microscopy using tightly focused radially polarized light," Opt. Lett., vol. 34, pp. 1870-1872 (2009).
[10] Bin Zhou, Liang Wang, Liu Liu, Fenfen Lei, “All-optical-fiber orbital angular momentum mode generator with a helical phase disk inserted between fibers,” IEEE Photonics Journal, vol. 7, no. 6, pp. 1-7, 2015.
[11] G. Ruffato, M. Massari, F. Romanato, "Diffractive optics for combined spatial-and mode-division demultiplexing of optical vortices: design, fabrication and optical characterization," Sci. Rep., vol. 6, 24760, 2016.
[12] G. Machavariani, Y. Lumer, I. Moshe, A. Meir and S. Jackel, "Efficient extracavity generation of radially and azimuthally polarized beams," Opt. Lett., vol. 32, pp. 1468-1470, 2007.
[13] R. Zhou, B. Ibarra-Escamilla, J. W. Haus-Peter, E. Powers and Q. Zhan, "Fiber laser generating switchable radially and azimuthally polarized beams with 140 mW output power at 1.6 μm wavelength," Appl. Phys. Lett., vol. 95, 191111, 2009.
[14] D. Lin, J. M. O. Daniel, M. Gecevičius, M. Beresna, P. G. Kazansky and W. A. Clarkson, "Cladding-pumped ytterbium-doped fiber laser with radially polarized output," Opt. Lett., vol. 39, pp. 5359-5361, 2014.
[15] T. Hirayama, Y. Kozawa, T. Nakamura and S. Sato, "Generation of a cylindrically symmetric, polarized laser beam with narrow linewidth and fine tunability." Opt. Express, vol. 14, pp. 12839-12845, 2006.
[16] C. Jocher, C. Jauregui, C. Voigtländer, F. Stutzk, S. Nolte, J. Limpert, and A. Tünnermann, "Fiber based polarization filter for radially and azimuthally polarized light." Opt. Express, vol 19, pp. 19582-19590, 2011.
[17] Zhongxi Lin; Anting Wang; Lixin Xu; Biao Sun; Chun Gu; Hai Ming, “Analysis of Generating Cylindrical Vector Beams Using a Few-Mode Fiber Bragg Grating,“ J. Lightwave technol., vol. 30, no. 22, pp. 3540-3544, 2012.
[18] S. Savin, M. J. F. Digonnet, G. S. Kino, and H. J. Shaw, "Tunable mechanically induced long-period fiber gratings," Opt. Lett., vol. 25, pp. 710-712, 2000.
[19] A. Witkowska, S. G. Leon-Saval, A. Pham, and T. A. Birks, "All-fiber LP_{11} mode convertors," Opt. Lett., vol 33, pp. 306-308, 2008.
[20] S. Ramachandran, P. Kristensen and M. F. Yan, "Generation and propagation of radially polarized beams in optical fibers." Opt. Lett., vol. 34, pp. 2525-2527, 2009.
[21] E. Alcusa-Sáez, A. Díez, and M. V. Andrés, "Accurate mode characterization of two-mode optical fibers by in-fiber acousto-optics," Opt. Express, vol. 24, pp. 4899-4905, 2016.
[22] W. Zhang, L. Huang, K. Wei, P. Li, B. Jiang, D. Mao, F. Gao, T. Mei, G. Zhang and J. Zhao, "Cylindrical vector beam generation in fiber with mode selectivity and wavelength tunability over broadband by acoustic flexural wave." Opt. Express, vol. 24, pp. 10376-10384, 2016.
[23] Biao Sun, Anting Wang, Lixin Xu, Chun Gu, Zhongxi Lin, Hai Ming, and Qiwen Zhan, "Low-threshold single-wavelength all-fiber laser generating cylindrical vector beams using a few-mode fiber Bragg grating," Opt. Lett., vol. 37, pp. 464-466, 2012.
[24] Biao Sun, Anting Wang, Lixin Xu, Chun Gu, Yong Zhou, Zhongxi Lin, Hai Ming, and Qiwen Zhan, "Transverse mode switchable fiber laser through wavelength tuning," Opt. Lett., vol. 38, pp. 667-669, 2013.
[25] Yong Zhou, Anting Wang, Chun Gu, Biao Sun, Lixin Xu, Feng Li, Dick Chung, and Qiwen Zhan, "Actively mode-locked all fiber laser with cylindrical vector beam output," Opt. Lett., vol. 41, pp. 548-550, 2016.
[26] Kokubun and K. Iga, "Single-mode condition of optical fibers with axially symmetric refractive index distribution," Radio Science, vol. 17, pp. 43-49, 1982.